Rebound map for water drop impacts on tilted surfaces

F. Villa, C. Antonini, I. Bernagozzi, N. Ongari, M. Marengo*
Department of Industrial Engineering, Università degli Studi di Bergamo,
Viale Marconi 5, 24044 Dalmine (BG), Italy.

Abstract

Normal and oblique impacts of water drops on dry solid surfaces were studied experimentally, to investigate the conditions for drop rebound. Data from literature suggest that rebound of a drop from a surface can be achieved when wettability is low, i.e. when contact angles, measured at the triple line (solid-liquid-air), are high. However, no clear criterion exists to predict when a drop will rebound from a surface, and which is the key wetting parameter to govern drop rebound (e.g. the "equilibrium" contact angle, θ_{eq}, the advancing , θ_A, or the receding, θ_R, contact angles, contact angle hysteresis, $\Delta\theta$, or any combination of these parameters). As such, experimental tests were conducted to study impacts of millimetric water drops on different dry solid surfaces with variable wettability (i.e. with variable θ_A, θ_R, and $\Delta\theta$), on hydrophobic and superhydrophobic surfaces. The study was focused at performing a phenomenological investigation of drop impact, at understanding in which conditions a drop rebound, and at evaluating drop rebound time (time shift between impact and detachment of the drop from the surface). Impacts were performed on horizontal and tilted surfaces, to evaluate the effect of surface inclination on drop impact outcome. Experimental conditions were: impact speed in the range $0.8 < V < 4.1\text{m/s}$, constant drop diameter $D_0 = 2.55\text{mm}$ (constant), Weber numbers in the range $25 < We < 585$, Ohnesorge number $Oh = 0.0022$ (constant), surface advancing contact angles $108° < \theta_A < 169°$, and receding contact angles $89° < \theta_R < 161°$, and surface inclination angle $0° < \alpha < 80°$.

For normal impact tests, it was found that receding contact angle is the key wetting parameter to control drop rebound: drop rebound was observed only on surfaces with receding contact angle is higher than ~100°; also, drop rebound time decreases monotonically by increasing receding contact angle; a drop rebound map was proposed, accordingly. The analysis of oblique impacts onto tilted surfaces led to the definition of six different impact regimes. Also, the following was found: on SHS ($\theta > 150°$, $\Delta\theta < 10°$), surface inclination generally enhances drop rebound and shedding from the surface, reducing drop rebound time up to 30%; on hydrophobic surfaces (with receding contact angles higher than ~100°), rebound was never observed for surface inclination up to 45°; the maximum inclination, $\alpha_{\max}$, at which drops rebound was found to depend on impact Weber number.

Introduction

Water repellency of natural and artificial superhydrophobic surfaces has been increasingly attracting the scientific and industrial community in the last years. Understanding the static and dynamic behavior of water on water repellant surfaces is not only a multidisciplinary scientific challenge across the complex fields of fluid mechanics and surface chemistry, but also has a high potential for several applications. Indeed, application of water repellant surfaces would be favorable in many fields, where water collection occurs as a consequence of impacting water drops. For example, in icing conditions, where impacted drops may stick to the surface and freeze, causing ice accretion [1]; on car glasses, where visibility is reduced while raining.

The property of "superhydrophobicity" is usually attributed to surfaces with high contact angles (>150°) and low contact angle hysteresis (<10°): note that these limits are arbitrary and are meant only to provide a reference. Superhydrophobic surfaces (SHS) show the highest potential for water shedding and self-cleaning capabilities. On a SHS, water drops show a very high mobility; also, impacting water drops can typically rebound from the surface in a short time after impact (few milliseconds). However, application of a SHS can present some potential critical issues, which can adversely affect its function as a water repellent surface. This is especially true, where dynamic systems such as drop impact are considered: e.g. considering the standard scientific vision, transition from a Cassie-Baxter to Wenzel state [2]-[3] is usually invoked to explain why a drop remains stuck on the surface, unable to rebound. Another critical issue, not addressed in the present paper, is related to the inferior mechanical durability of a SHS. As such, from an engineering perspective, there may be occasions, where application of a good hydrophobic surface (i.e. contact angles of 90°-120° and moderate contact angle hysteresis 10°-20°) can adequately satisfy the required performance criteria (e.g. drop

* Corresponding author: marco.marengo@unibg.it

rebound/shedding from the surface). In order to provide guidelines for the choice of a hydrophobic/superhydrophobic surface, based on the specific conditions of application, fundamental drop impact studies are needed to investigate the mechanisms of drop rebound, to identify which are the controlling parameters for rebound (in terms of both surface properties and fluid mechanic parameters) and to define a rebound map, for normal and oblique impacts.

Water drop rebound after normal impact on a surface with low wettability has been widely studied by several groups [2]-[13], after the first pioneering work by Hartley and Brunskill [14]. In [14], an energy balance approach for drop deformation after impact was proposed, accounting wettability through the value of a static contact angle. In 1997, Mao *et al.* [15] studied impact on surfaces with equilibrium contact angle $37° < \theta_e < 97°$; they proposed a rebound criterion, based on the estimation of drop "excess rebound energy", E_{ERE}, which is derived semi-empirically as function of drop maximum spread factor, $\xi_{\max}$, and surface equilibrium contact angle, θ_e:

$$E_{ERE} = \frac{1}{4}\xi_{\max}^2\left(1-\cos\theta\right) - 0.12\xi_{\max}^{2.3}\left(1-\cos\theta\right)^{0.63} + \frac{2}{3}\xi_{\max}^{-1} - 1 \qquad (1)$$

According to Mao *et al.*, drop rebounds from the surface for $E_{ERE} > 0$, otherwise drop will remain attached to the surface. Using Eq. 1, it was concluded that drop rebound can be observed for equilibrium contact angles higher than 90°, and the tendency of drop rebound increases as the maximum spread increases (e.g. by increasing impact speed, V) and the contact angle increases.

Drop rebound time [16] (i.e. time between impact and rebound instants, also referred to in literature as residence time [17] or contact time [5]) on SHS was found by Quéré and co-workers [5]-[6] to be and function of drop mass, m, and liquid surface tension, σ, and independent from impact speed, V:

$$t_R = 2.6\left(\rho D_0^3/8\sigma\right)^{1/2} \qquad (2)$$

where ρ is density, and D_0 drop initial diameter. The value of rebound time is close to the first-order vibration period of a freely oscillating drop [21], the so called Rayleigh time:

$$t_{Rayleigh} = \pi/\sqrt{2}\left(\rho D_0^3/8\sigma\right)^{1/2} \qquad (3)$$

the only difference being the numerical pre-factor. The similarity between rebound and Rayleigh time was first reported by Watchers and Westerling [17] for the case of drop impacting on a hot surface in Leidenfrost conditions. In [4], the contact time was found to increase (typically by a factor of 2) at small impact velocities (in the order of 5-20 cm/s for millimetric drops), which was interpreted as the result of the drop weight, since gravity effect cannot be neglected for small impact speeds.

In [8], Rioboo *et al.* proposed a schematic drop impact regime map, identifying four different outcomes: deposition, rebound, sticking, and fragmentation. For the specific system analyzed (water drops on superhydrophobic polypropylene surface), the transition from rebound to fragmentation was found to be governed by Weber number, $We = \rho V^2 D_0/\sigma$; the threshold value between two regimes was found to be $We \approx 60$. For the deposition-rebound limit, it was experimentally observed in [8] that the transition does not only depend on the Weber number, but also on two wetting parameters: the average contact angle, θ_{AV}, defined as the average between advancing, θ_A, and receding, θ_R, contact angles, and the contact angle hysteresis, $\Delta\theta$. This is an important result, which stresses the need of characterizing a surface by means of advancing and receding contact angles (as already discussed in another previous study by Šikalo *et al.* [18]), and tries to correlate such measurement to drop impact dynamics. The interested reader may deepen the topic of wettability characterization, and in particular why it is more appropriate to provide a range for the contact angles (i.e. provide advancing and receding contact angles), rather than a single value for the "equilibrium" contact angle, in [19], a paper containing a deliberately provocative statement in the title: "Teflon is hydrophilic", and the following discussions (e.g. [20]).

Li *et al.* [11] investigated the effect of surface texturing on the receding phase and thus drop contact time. Performing tests on textured silicon surfaces, decorated by square arrays of pillars with different geometries, they showed that surface texture has a direct effect on receding contact angle, thus modifying retraction dynamics and, in case of rebound, drop rebound time.

With respect to drop impact on tilted surface, to the authors' knowledge, the only systematic experimental study of single drop impact on dry tilted surface is [22]. In this study, the phenomenology of drop impact was addressed for surfaces with various wettability with $10° < \theta_A < 105°$ and $6° < \theta_R < 95°$ for water (the most hydrophobic surface was a smooth wax surface). It was found that for high surface inclination ($\alpha > 80°$), drop rebound from the most hydrophilic tested surface (smooth glass, $R_a = 0.003\mu m$) when normal Weber number, We_N (computed using normal speed, V_N, as reference speed) is lower than a critical value, We_{Ncr}, which ranges from 1 (water and glycerin) to 3

(isopropanol). This particular rebound was explained assuming that, for low normal Weber numbers, the drop and the target plate do not make contact due to the presence of a thin air film which acts as a barrier to deposition. Rebound was never observed nor on rough glass ($R_a = 3.6\mu m$) and wax ($R_a = 0.3\mu m$), which have roughness higher than the critical typical value for air film thickness, in the order of $0.1\mu m$ [23].

With respect to the available literature on drop rebound, the present paper illustrates the first systematic experimental study on drop impact on hydrophobic and superhydrophobic surfaces, that includes normal as well as oblique impacts. Aim of the study is to provide phenomenological observation of drop impacts on water repellant surfaces (with equilibrium contact angles higher than 90°) and to understand the mechanism of drop rebound. Particular attention was focused in identifying which wetting parameter(s) (i.e. the advancing, θ_A, or the receding, θ_R, contact angles, or contact angle hysteresis, $\Delta\theta$) control(s) drop rebound, and to provide an impact regime map. The analysis of oblique impacts will allow evaluating the effect of a surface inclination (which introduces a tangential speed and a tangential force, i.e. gravity component parallel to the surface) on drop impact outcome and drop rebound time, in case rebound occurs.

Experimental Methods

Eight surfaces with different wetting parameters were produced, characterized by means of sessile drop method (i.e. measuring the advancing, θ_A, and receding, θ_R, contact angles, while expanding quasi-statically and contracting a drop on a horizontal surface) and tested in drop impact experiments. The surface used were the following: (i) A1-Teflon, (ii) A2-Teflon; (iii) B1-PP; (iv) B2-PP, (v) SHS-FAS, (vi) SHS-Teflon, (vii) SHS-CNR1, (viii) SHS-CNR2. Surface (i) to (iv) are smooth hydrophobic surfaces (with roughness lower than 500nm), whereas surfaces (v) to (viii) are textured superhydrophobic surfaces (roughness ~2-5μm). Surfaces (i) and (ii) are Teflon coated glasses, and surfaces (iii) and (iv) are thin polypropylene layers deposited on glass, which serve as rigid substrate (more details of surfaces (i) to (iv) can be found here [24]). SHS-FAS was fabricated by means of a one-step wet reaction, by treating an aluminum sample in a water solution of sodium hydroxhyde and perfluoroctyltriethoxysilane (FAS). SHS-Teflon was fabricated on an aluminum substrate by aluminum etching in acid solution (to achieve the desired surface roughness) and subsequent spraying with Teflon® (10:1 v/v solution of FC-75 and Teflon® from DuPont™). Surfaces (vii) and (viii) were produced using a fluorinated molecule (no details on surface fabrication can be provided due to confidentiality).

Table 1 reports the values of advancing and receding contact angles, their difference, which is known as contact angle hysteresis ($\Delta\theta$). All eight surfaces have been tested for normal impact tests, and four of them (A1-Teflon, A2-Teflon, SHS-FAS, SHS-Teflon) were selected (on the basis of drop rebound performance in normal impact tests) and tested also for oblique impact tests.

Table 1: Advancing (θ_A) and receding (θ_R) contact angles, contact angle hysteresis ($\Delta\theta$), surface mean roughness, R_a, and rms roughness, R_q, for all tested surfaces. Typical standard deviation for contact angles is ±3°.

	surface	θ_A **[°]**	θ_R **[°]**	$\Delta\theta$ **[°]**	**normal impacts**	**oblique impacts**
i	A1-Teflon	111	104	7	x	x
ii	A2-Teflon	121	108	13	x	x
iii	B1-PP	108	91	17	x	
iv	B2-PP	113	89	24	x	
v	SHS-FAS	169	161	8	x	x
vi	SHS-Teflon	160	145	15	x	x
vii	SHS-CNR1	156	155	1	x	
viii	SHS-CNR2	163	154	11	x	

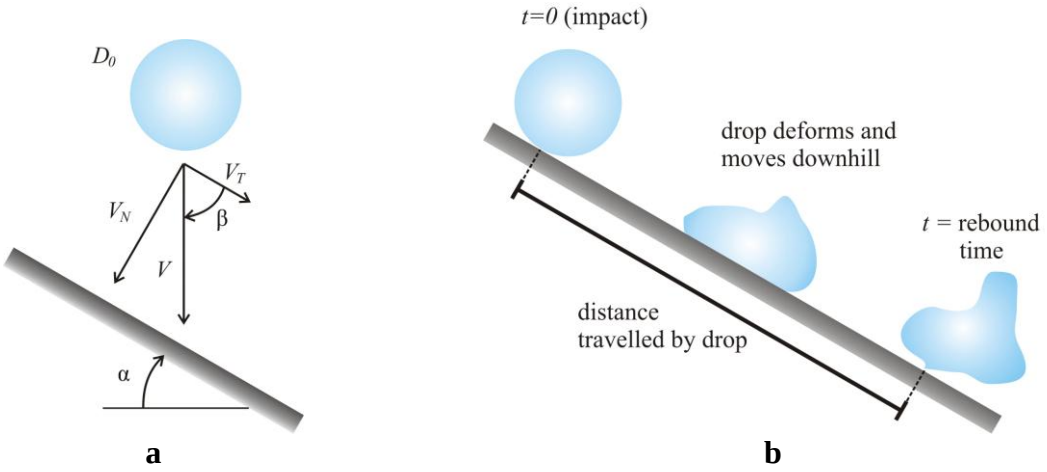

Figure 1: Schematic of drop impact on a tilted surface: a) drop before impact, with indication of the principal impact parameters; b) schematic of drop evolution and parameter of interests.

A typical experimental apparatus for drop impact studies was used, in which a drop is generated at the tip of a needle, then is accelerated by gravity and impacts on the dry solid surface, which can be inclined from α equal to 0° (horizontal surface) to ideally 90° (vertical surface) – see Figure 1. Experimental conditions were: impact speed in the range $0.8 < V < 4.1\text{m/s}$, constant drop diameter $D_0 = 2.55\text{mm}$ (constant), Weber numbers in the range $25 < We < 585$, Ohnesorge number $Oh = 0.0022$ (constant), surface advancing contact angles $108° < \theta_A < 169°$, and receding contact angles $89° < \theta_R < 161°$, and surface inclination angle $0° < \alpha < 80°$. A practical maximum limit for surface inclination ($\sim 80°$) was found, due to the difficulty in capturing entirely the drop trajectory and its dynamics. Images of drop impact were recorded using a high-speed camera (PCO 1200-hs) with a typical frame rate of 1015fps and pixel resolution in the range 30-35μm (all this visualization parameters represent the best compromise between spatial and temporal resolution, and field of view). To record drop impact events, images were taken from the side, with the same view as illustrated in Figure 1 (camera direction is perpendicular to the symmetry plane of the impacting drop). This view was chosen as the most suitable, since it allows to measure the following parameters: i) drop rebound time, i.e. the time shift between drop impact and drop lift-off from the surface (also known as contact time); ii) visualize the movement of the contact line at the downhill and uphill fronts. Note that the camera is mounted on the same support of the surface, and rotate rigidly with it, to optimize the observation window. Images were manually analyzed to identify the drop impact outcome and eventually measure drop rebound time, in case rebound occurs. Rebound time was measured manually, since the presence of prompt splash and/or break-up, characterized by secondary drop ejection (which occurs in the majority of tested cases, especially for SHS), does not allow to perform an automatic measure.

Results and Discussion

A. Drop normal impacts (horizontal surface)

Drop impact tests on horizontal surfaces ($\alpha = 0°$) showed that drop (full) rebound occurs on the following surfaces: A1-Teflon, A2-Teflon, SHS-FAS, SHS-Teflon, SHS-CNR1 and SHS-CNR2. Drop never rebounds on B1-PP and B2-PP. Also, rebound time was found to be independent from impact speed, V, not only for SHS surfaces, as predicted by Quéré and co-workers [8], but also for hydrophobic surfaces (A1-Teflon and A2-Teflon). However, rebound time, t_R, is not the same far all surface, but depends on surface wettability: in particular, rebound time was found to correlate well to receding contact angle, θ_R. Figure 2 illustrates the dependence of t_R on θ_R; data show a clear trend: drop rebound time decreases monotonically with increasing receding contact angle. The three best SHS surface (SHS-FAS, SHS-CNR1 and SHS-CNR2), which have receding contact angles higher than 150°, show rebound time that are well predicted by Eq. 2, which gives a rebound time of ~14ms. On SHS-Teflon, receding contact angle is 145° and the rebound time increases to 16ms. For the two hydrophobic surfaces, A1-Teflon and A2-Teflon, rebound time increases to ~22ms.

In our previous study [12], we already showed that for a hydrophobic /superhydrophobic surface the spreading time is ~3ms at moderate Weber numbers ($We < 200$) and decreases when increasing Weber number for $We > 200$. This

confirms that the differences on t_R between surfaces have to be found in the recoil phase, which lasts for ~10-13ms on SHS and ~19ms on A1-Teflon and A2-Teflon. This result highlights that, even at high speed impacts, with Weber number in the order of hundreds, wettability plays a dominant role in the recoiling phase, and that the knowledge of surface receding contact angle, which is measured quasi-statically, represent a valuable information for predicting the dynamic behaviour of a drop on a surface (for the impact conditions investigated here).

As an additional note, surface impalement, with transition from Cassie-Baxter to Wenzel state, occurs on none of the tested SHS, and drops rebound at all impact speeds in the investigated range.

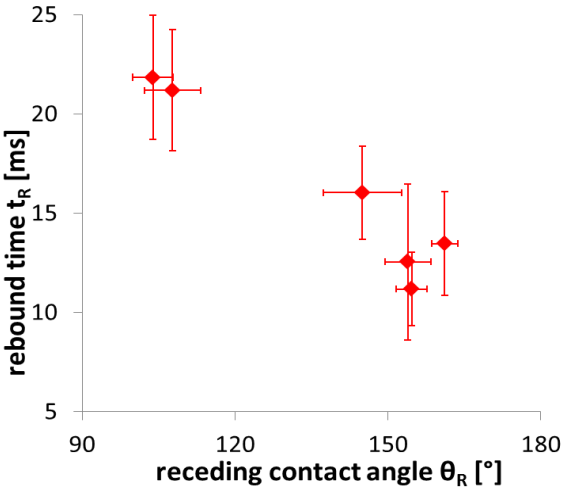

Figure 2: drop rebound time, t_R, for water drop impacting normally on a dry surface, as function of surface receding contact angle, θ_R. Data are obtained as average for all investigated impact speeds. The rebound time predicted by Eq. 2 for a SHS is ~14ms.

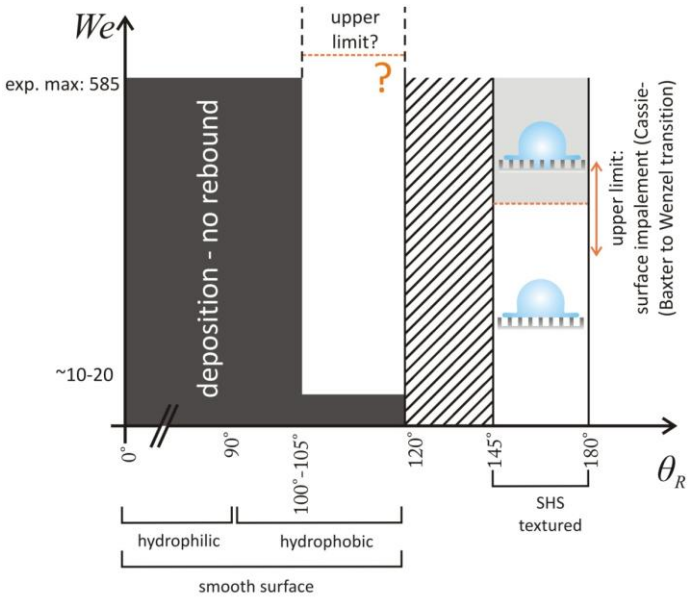

Figure 3: Schematic rebound map for water drops impacting normally on a surface, plotted on the $We-\theta_R$ plane. See text for discussion.

The identification of receding contact angle as the principal wetting parameter to control drop recoil and rebound allows defining a drop rebound map. Figure 3 illustrates a schematic representation of such map on the $We-\theta_R$ plane. On hydrophilic surfaces, which have contact angles low receding contact angles, rebound never occurs and the drop remain stuck on the surface. Rebound can be only observed for high receding contact angles. Data from present study show that drops do not rebound for $\theta_R \approx 90°$ (B1-PP and B2-PP), whereas they rebound on surfaces with $\theta_R \approx 105°$. Data from Šikalo *et al.* [22] show that drop was not rebounding on waxed surface with $\theta_R \approx 95°$. As such, we believe that $\theta_R \approx 100°$ represent the lower boundary to observe rebound. For hydrophobic surface, we observed there is a minimum limit for We, likely in the range 10-20, since gently deposited drops (falling height $h \approx 1\text{cm}$, corresponding to $We \approx 7$) do not rebound. With respect to SHS surfaces (surfaces with $\theta_R > 145°$ in the present study), no lower limit was found, since drops rebound even when gently deposited. Also, tested SHS surfaces do not have any upper limit in the investigated range (up to $We = 585$), but we know from other studies ([2],[9]) that a critical maximum velocity exist, above which impalement may occur in the vicinity of the impact point and inhibit drop rebound: the reason why drop does not rebound is that locally the wetting state changes, and the local receding contact angle typically decreases to values lower than 90° (typical of surfaces in Wenzel state). The area with $120° < \theta_R < 145°$ has been intentionally crossed because this area is difficult to explore: no smooth surface show contact angles higher than 120° and when a Cassie-Baxter wetting state is reached, receding contact angle are typically higher than 145°-150°.

B. Drop oblique impacts (tilted surface)

B1. Phenomenological observations

The first part of the study of oblique drop impacts involved the identification of principal drop impact outcomes. Five main outcomes where identified and are illustrated in Figure 4: a) deposition, when the drops deforms but remains in the impact area; b) slug, when drop core slides downhill, with the uphill edge that remains pinned or only poorly moves downhill; c) sliding, when the drop slides downhill (with the uphill edge moving together with the drop); d) rolling, when the drop rolls downhill (this is observed depositing drops SHS at high tilting inclination); e) partial rebound, when only a part of the drop detaches from the surface, while the other remain stuck (eventually slides downhill); f) full rebound. Other phenomena, such as prompt splash (typically on the downhill advancing front) or drop break-up, can be observed in combination with one of the above described outcomes.

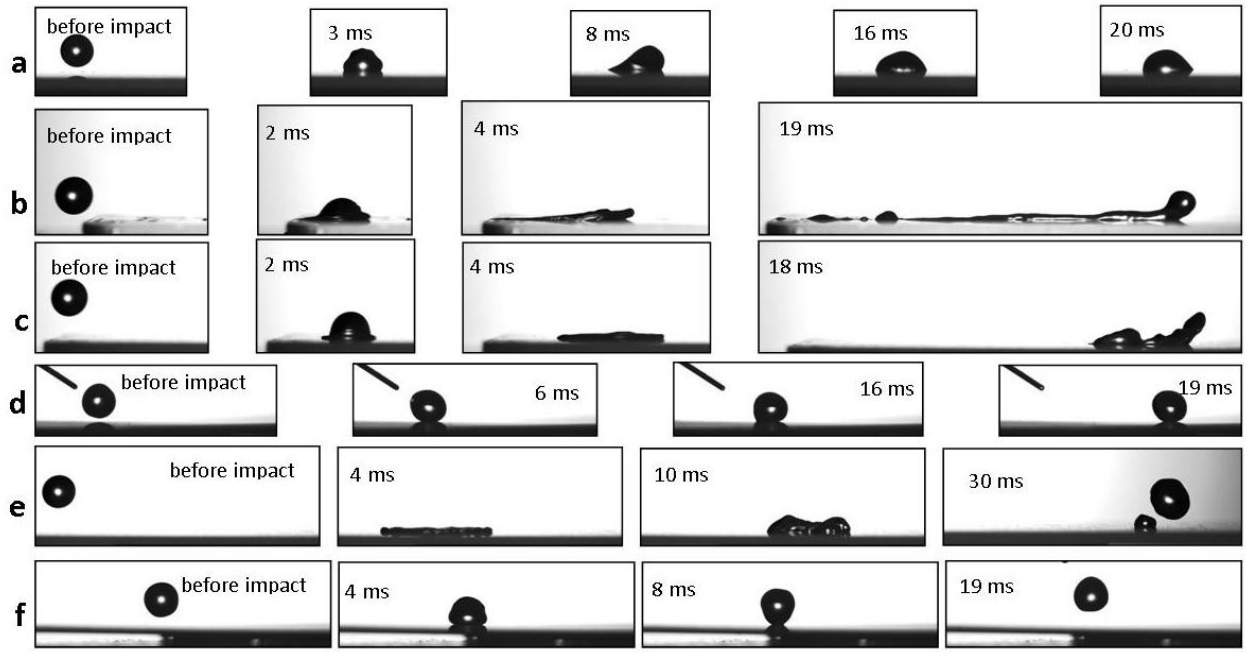

Figure 4: Outcomes of water drop impact onto various tilted substrates: (a) deposition on A2–Teflon (D_0=2.57 mm, V=0m/s, α=45°); (b) slug on A1–Teflon (D_0=2.57 mm, V=2.36 m/s, α=70°); (c) sliding on A2–Teflon (D_0=2.57 mm, V=2.36 m/s, α=60°); (d) rolling on SHS-FAS (D_0=2.57 mm, V=0 m/s, α=60°); (e) partial rebound on A2–Teflon (D_0=2.57 mm, V=2.36 m/s, α=45°); (f) rebound on SHS-FAS (D_0=2.57 mm, V=0 m/s, α=10°).

B2. Drop rebound time on SHS

On the two SHS tested for oblique impacts (SHS-Teflon and SHS-FAS), drop rebound was observed for all impact conditions. Figure 5 illustrates the values of drop rebound time, t_R, as function of surface tilt angle, α, at different impact Weber numbers, We, for SHS-Teflon surface. Two different trends can be recognized: for $We \geq 199$, surface inclination has a positive effect on drop shedding, with a reduction of drop rebound time from ~16ms (at $\alpha = 0$) to values of ~9ms (reduction of ~40%) at the highest inclination. For the three lowest values of tested Weber numbers ($We \leq 81$), rebound time initially decreases, but the increases to higher values, reaching a maximum for the highest observed contact angle. This effect, which is still under investigation, should be probably attributed to low normal impact velocities, V_N, as already shown in [4] for normal drop impact at very low impact speeds ($V_N = V \approx 5-20\text{cm/s}$).

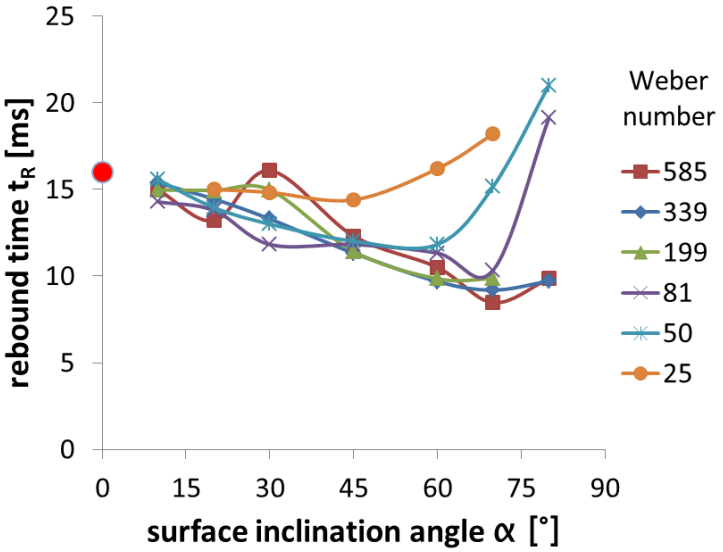

Figure 5: Drop rebound time on one tested SHS-Teflon as function of surface inclination, α, at different Weber number (see legend), calculated using the impact speed, V. Standard deviation for rebound time is ±1.5ms.

B3. Drop impact on tilted hydrophobic surface

The analysis of impacts on tiled hydrophobic surfaces provide valuable information, because four out of six different impact outcomes can be observed: rebound, partial rebound, sliding and slug. The impact outcome map is illustrated in Figure 6, where different outcomes are identified on the $We-\alpha$ plane, for water drops impacting on A2-Teflon Drop rebound occurs at all tested Weber numbers for $\alpha \leq 10°$. By increasing α, the critical We above which drop does not rebound is observed to monotonically decreases. Drop full rebound was observed up to $\alpha \leq 45°$. As a general trend, by increasing We and α (i.e. moving from bottom-left to top-right in Figure 6), the drop outcome progressively passes from drop rebound, to an intermediate region where partial rebound and sliding occur, and finally to slug, which is found at the highest surface inclination, i.e. when $We_T > 3We_N$. As such, the trend for hydrophobic surfaces appear different than on SHS: on SHS, drop rebound always occurs on tilted surface, increasing the tilt angle generally facilitates drop shedding and reduce droop rebound; differently on a smooth hydrophobic surface no rebound can be observed above a certain surface inclination. With respect to surface inclination effect on drop rebound time, no particular trend was identified for impacts on tilted A2-Teflon (figure not reported for brevity).

A key issue for drop rebound might be the recoil phase and its dynamics. By increasing the tangential velocity, the rear front may not be able to recoil fast enough to make the contact line collapse and to allow drop rebound. This effect (related to contact line dynamics) becomes predominant at high inclination angle $\alpha > 45°$, inhibiting drop rebound.

Summary and Conclusions

This paper presents results of a drop impact study on hydrophobic and superhydrophobic surfaces, where both normal and oblique impacts were analyzed for the first time.

The analysis of drop impact on horizontal surfaces highlighted the role of the receding contact angle in governing the drop rebound from a surface: rebound can be observed only on surfaces where the receding contact angle is higher than 100°. Also, rebound time decreases for increasing receding contact angles. Accordingly, a rebound map for impacts on horizontal surfaces has been proposed.

Analysis of impacts on tilted surfaces has allowed to identify six different impact outcomes: deposition, slug, sliding, rolling, partial rebound, rebound. Drop impact analysis has also led to two main findings: for drop impact on SHS ($\theta_R > 145°$), surface inclination facilitates drop shedding and allows reducing rebound time up to 30%; on hydrophobic surfaces, increasing surface inclination leads to a transition from drop rebound, to partial rebound and sliding, and finally to slug (at high Weber number and surface inclinations).

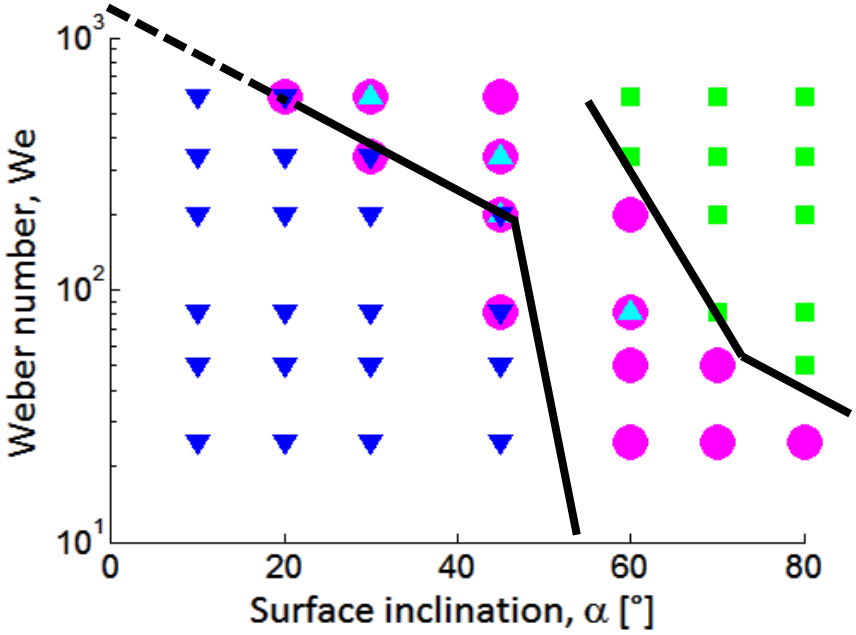

Figure 6: Drop map on one tested hydrophobic surface (A2-Teflon), plotted on the plane $We-\alpha$. Lines to separate different regions are to guide the eyes.

Acknowledgements

The authors acknowledge Regione Lombardia for funding the project "Strumenti innovativi per il progetto di sistemi antighiaccio per l'aeronautica" (within the Framework Agreement) and AleniaAermacchi for financial support. The author also thank D. Barona, H. Chen, A. Amirfazli (University of Alberta, Canada) for providing surfaces (i)-(iv) and (vi), and M. Raimondo (ISTEC CNR, Italy) for providing surfaces (vii) and (viii).

References

[1] C. Antonini, M. Innocenti, T. Horn, M. Marengo, and A. Amirfazli, *Cold Reg. Sci. Tech.* 67: 58–67 (2011)
[2] D. Bartolo, F. Bouamrirene, É. Verneuil, A. Buguin, P. Silberzan, and S. Moulinet, *Europhys. Lett.*, 74: 299 (2006)
[3] M. Reyssat, A. Pepin, F. Marty, Y. Chen, and D. Quéré, *Europhys. Lett.*, 74: 306–312 (2006)
[4] K. Okumura, F. Chevy, D. Richard, D. Quéré and C. Clanet, *Europhys. Lett.*, 62: 237–243 (2003)
[5] D. Richard, C. Clanet, and D. Quéré, *Nature* 417: 811 (2002)
[6] C. Clanet, C. Béguin, D. Richard, and D. Quéré, *J. Fluid Mech.* 517: 199–208 (2004)
[7] A.L. Biance, F. Chevy, C. Clanet, G. Lagubeau, and D. Quéré, *J. Fluid Mech.* 554, 47–66 (2006)
[8] R. Rioboo, M. Voué, A. Vaillant, and J. De Coninck, *Langmuir* 24: 14074-14077 (2008)
[9] P. Brunet, F. Lapierre, V. Thomy, Y. Coffinier and R. Boukherroub, *Langmuir* 24: 11203–11208 (2008)
[10] M. Lee, Y. S. Chang, and H.-Y. Kim, *Phys. Fluids* 22: 072101 (2010)
[11] X. Li, X. Ma, Z. Lan, *Langmuir* 26: 4831–4838 (2010)
[12] C. Antonini, A. Amirfazli, and M. Marengo, *ILASS Brno*, Czech Reupblic, Sept. 2010
[13] Y. C. Jung and B. Bhushan, *Langmuir* 24: 6262-6269 (2008)
[14] G. Hartley, R. Brunskill. In: *Surface Phenomena in Chemistry and Biology* (ed. J. F. Danielli), 214–223. Pergamon, 1958
[15] T. Mao, D. C. S. Kuhn, and H. Tran, *AIChE Journal* 43: 2169-2179 (1997)
[16] S. Chandra, and C.T. Avedisian, *Proc. Roy. Soc. Lond A* 432: 13-41 (1991)
[17] L.H.J. Wachters, and N.A.J. Westerling, *Chem. Eng. Sci.* 21: 1047-1056 (1966)
[18] Š. Šikalo, C. Tropea, M. Marengo, and E. N. Ganić, *Euro Conference -Renewable Technologies for Sustainable Development*, Madeira Island, Portugal, 26-29 June 2000
[19] L. Gao and T. J. McCarthy, *Langmuir* 24: 9183–9188 (2008)
[20] G. McHale, *Langmuir* 25: 7185–7187 (2009)
[21] Lord Rayleigh, *Proc. R. Soc. Lond. A* 29: 71–97 (1879)
[22] Š. Šikalo, C. Tropea, and E.N. Ganić, *J. Colloid Interf. Sci.* 286: 661–669 (2005)
[23] V.V. Poddubenko and R.M. Yablonik, *Fluid Mech. Sov. Res.* 19 (1990)
[24] H. Chen, T. Tang, and A. Amirfazli, *submitted to Colloid Surface A.*
[25] A.L. Yarin, *Annu. Rev. Fluid Mech.* 38: 159–192 (2006)
[26] R. Rioboo, M. Marengo, and C. Tropea, *Exp. Fluids* 33:112–124 (2002)